55th International Conference on Environmental Systems
12-16 July 2026, Rio Grande, Puerto Rico
ICES-2026-492

Harness Thermal Heat Loss Measurement for a Lunar Surface-Deployed LEMS Artemis III Payload

Ethan Burbridge*
Vertex Aerospace, LLC, Grasonville, MD 21638

Brian Langbein†
NASA Goddard Space Flight Center, Greenbelt, MD, 20771

Juan Rodriguez-Ruiz ‡
NASA Goddard Space Flight Center, Greenbelt, MD, 20771

and

Elliot Schwartz§
NASA Goddard Space Flight Center, Greenbelt, MD, 20771

The Lunar Environment Monitoring Station (LEMS) is an autonomous, survive-the-lunar-night seismic suite to be deployed on the Lunar surface by the Artemis III crew and designed to operate continuously for two years. It will see the extremes of the Lunar south pole thermal environment where surface temperatures range from -200°C to +20°C and where nighttime duration is at least 354 hours. Given power and mass constraints, the thermal system is limited to 2.5 Watts of heat during the lunar night. The electrical harnessing named the Signal and Power Passthrough (SAPP) was designed to minimize heat loss while meeting power and signal integrity requirements. To mitigate risk due to uncertainty associated with the harnessing materials, routing, and tie-downs, a flight-like thermal conductance test was performed to measure the heat loss. The test methodology, results, and model correlation are presented.

I. Acronyms and Nomenclature

GSE	=	Ground Support Equipment
I_i	=	Current Measurement
LEMS-A3	=	Lunar Environment Monitoring Station – Artemis 3
MLI	=	Multi-Layer Insulation
N	=	Number of measurement samples
PEEK	=	Polyether Ether Ketone
RRU	=	Risk Reduction Unit
SAPP	=	Signal and Power Passthrough
SD	=	Silicon Diode
TC	=	Thermocouple
TCS	=	Thermal Control Subsystem
V_i	=	Voltage Measurement
$\bar{x}$	=	Average of the sample period
x_i	=	Measurement
σ	=	Measurement uncertainty

* Thermal Engineer, Vertex Aerospace, LLC, and PO BOX 192, Grasonville, MD 21638
† Thermal Engineering Intern, Thermal Engineering Branch, and 8800 Greenbelt Rd Greenbelt, MD 20771
‡ Thermal Principal Design Lead, Thermal Engineering Branch, and 8800 Greenbelt Rd Greenbelt, MD 20771
§ Thermal Engineer, Thermal Engineering Branch, and 8800 Greenbelt Rd Greenbelt, MD 20771

I. Introduction

THE Lunar Environment Monitoring Station for Artemis 3 (LEMS-A3) requires a thermal control subsystem that minimizes heat losses to be able to survive and operate continuously through a nominal lunar night, equivalent to a 360-hour eclipse. Figure 1 shows the system architecture which is furthered detailed in a previous paper [1]. The battery is sized for to accommodate 2.3 W of continuous power dissipation during lunar night from electronics, instruments, and heaters.

The LEMS-A3 bus thermal control subsystem (TCS) has five primary heat loss paths: heat switched radiator, launch locks, blanketing, antenna coax cables, and flight harnessing. Because the seismometers are deployed in the lunar regolith, the electronics and heater power consumption in the seismometers are an additional power sink. The predicted heat leak contributions of each of these elements is captured in Table 1. The flight harnessing heat leak measured in this test is known as the Signal and Power Passthrough (SAPP).

Table 1: LEMS-A3 Predicted Heat Loss during Lunar Nighttime

Description	Cold Operational Predicted Heat Loss [W]
Bus Launch Lock	-0.483
Integrated Multi-Layer Insulation	-0.252
Signal and Power Passthrough	-0.223
Antenna Coax	-0.238
Radiator Heat Switch	-0.458
Bus Heat Loss	-1.654
Bus Internal Electronics CBE Heat	1.082
Bus Heater (GSE Heater) Power	0.578
Total Internal Electronics Power	1.660
Seismometer-1 As-Measured Power	0.330
Seismometer-2 As-Measured Power	0.330
Total LEMS Power Consumption	2.320

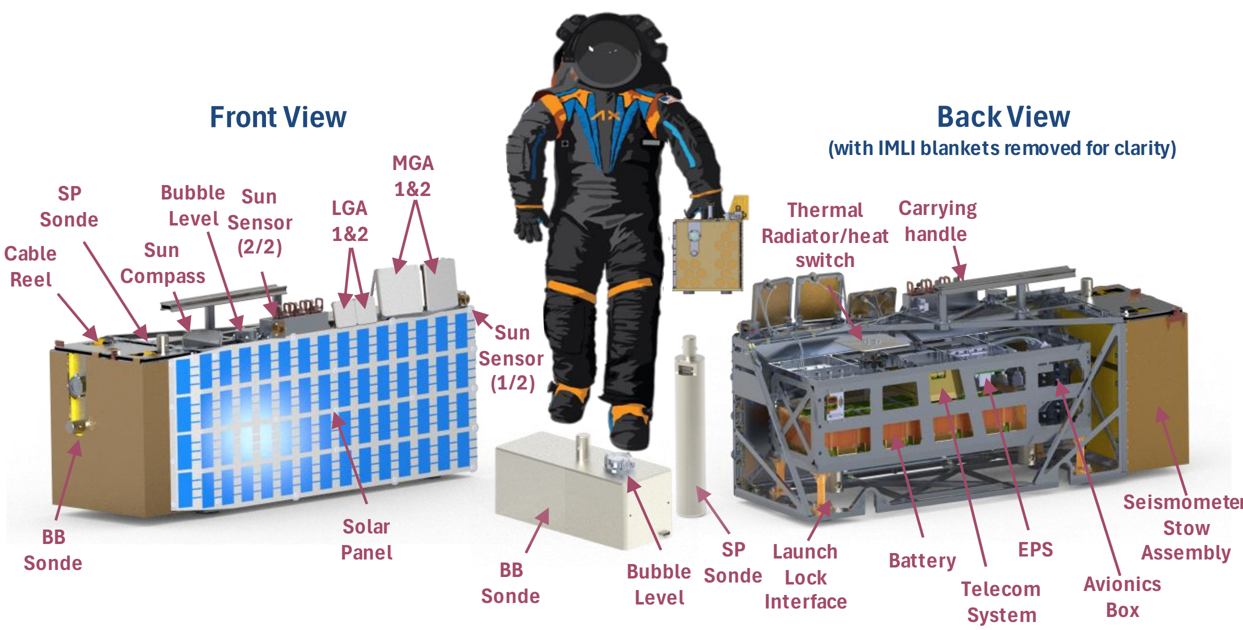

Figure 1: LEMS-A3 flight configuration showing seismometers and astronaut carry for surface deployment

II. Thermal Conductance Test Configuration and Methodology

A. Test Objectives

The SAPP thermal conductance test was conducted to mitigate the risk of excessive heater power demand during lunar night operations, which could result in premature depletion of the LEMS-A3 battery. During lunar night operations, internal electronics are actively heater-controlled while external components reach temperatures approaching −200 °C. The SAPP harness directly couples the warm internal hardware to the cold external environment, so accurate knowledge of the heat loss is necessary to ensure lunar night survivability. If this heat leak exceeds predictions, additional heater power would be required to maintain allowable internal temperatures, reducing the amount of time LEMS can survive the lunar night. Three primary test objectives were established from this mission-level risk.

The first objective was to measure and characterize the cold operational thermal conductance and total heat leak of a flight-like SAPP Risk Reduction Unit (RRU) under flight-like boundary conditions. The predicted heat leak is seen in Table 1 at -0.223 W. In flight, the SAPP is expected to have a gradient from -30°C inside the LEMS-A3 bus to -200°C outside at component connections and harness tie down bases. With that gradient, the assumed conductance is 1.3E-03 W/°C. Quantifying the steady-state heat flow from the warm internal interface to the cold external interface enables assessment of the harness thermal performance and provides an empirical basis for evaluating design margins.

The second objective was to obtain high-fidelity, independent thermal balance datasets to support correlation of the SAPP thermal model. Controlled thermal balance points with well-defined boundary conditions enable analysts to reconcile predicted temperatures and heat flows with measured values. Successful correlation improves confidence in model-based predictions of flight performance and strengthens the analytical foundation for mission-level power budgeting.

The third objective was to quantify the contribution of radiation heat transfer to the total cold operational heat leak. By incorporating flight-like multi-layer insulation (MLI) on the SAPP RRU and varying radiative boundary conditions during selected balance points, the test enabled separation of conductive and radiative heat transfer mechanisms. This information supports evaluation of the SAPP insulation architecture and informs potential design refinements.

Collectively, these objectives were structured to reduce uncertainty in the predicted SAPP heat leak, increase confidence in lunar night survival margins, and lower overall thermal control system risk for the LEMS mission.

B. Overview of Test Setup

The unit under test consisted of a flight-like SAPP RRU with representative harness routing, flight-like harness mounts, and flight-like MLI. Dedicated ground support equipment (GSE) established two distinct thermal zones within the thermal vacuum chamber: (1) a warm zone representing the heater-controlled internal LEMS environment, and (2) a Cold Zone representing the external lunar night environment.

The SAPP harness physically bridged these two zones, serving as the dominant thermal coupling between the warm inside and the cold outside. A schematic of the test configuration described is shown in Figure 2 (left); note that the temperatures called out refer to the nominal setpoints during the baseline conductance test phase. A higher-fidelity computer-aided design model of the test configuration is shown in Figure 2 (right). Photos of the test setup in the vacuum chamber are shown in Figure 3.

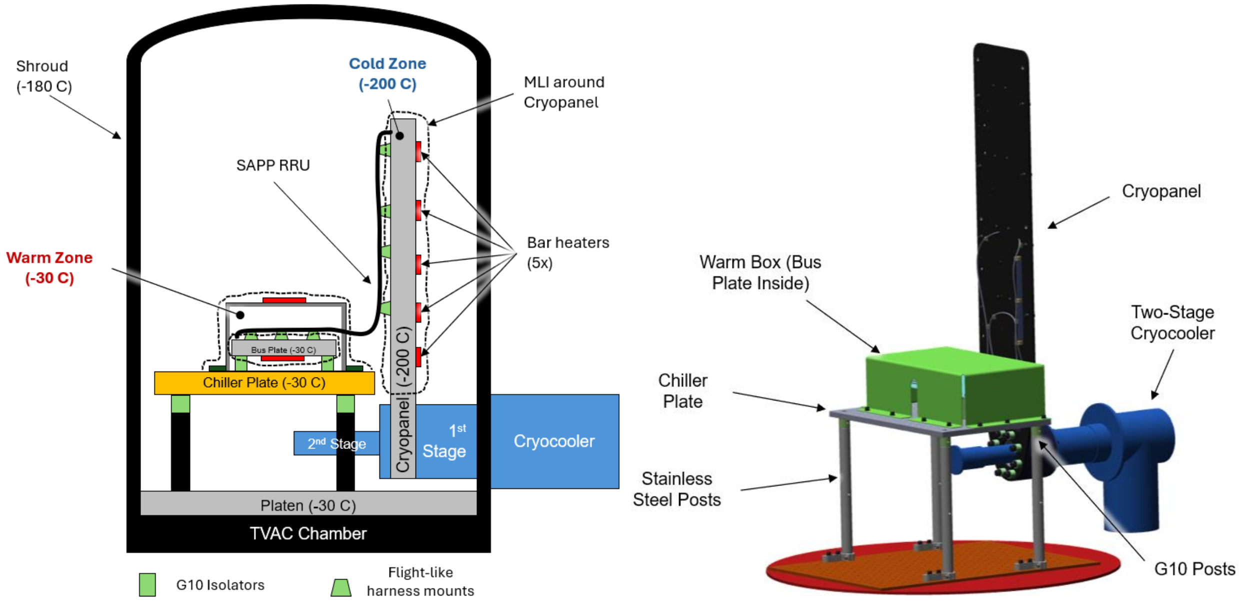

Figure 2: (left) Test block diagram. (right) Model of the test configuration.

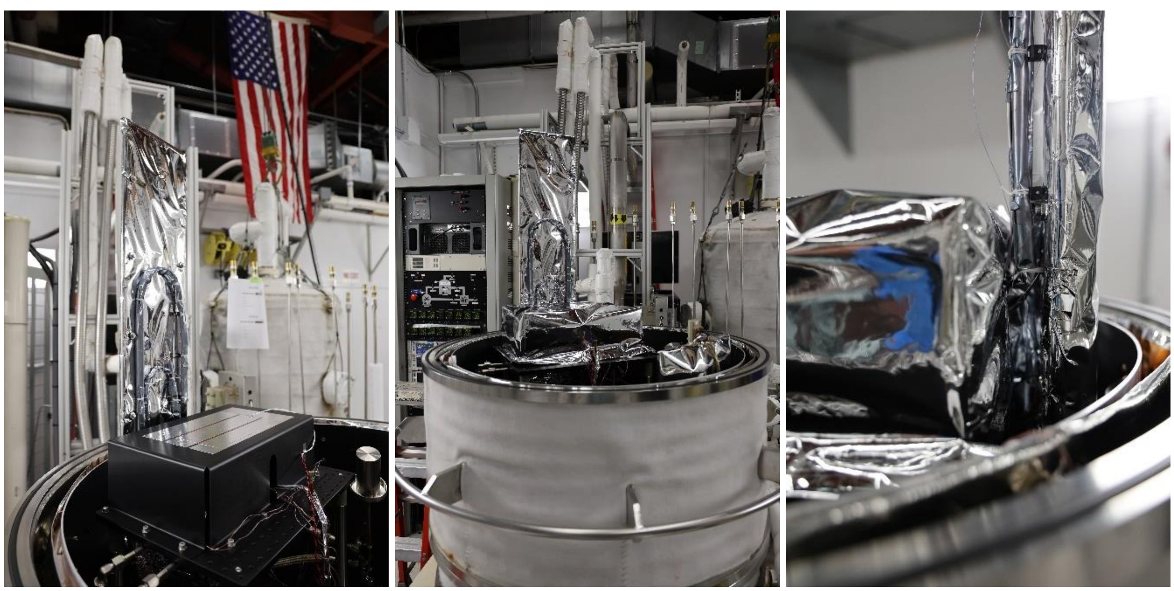

Figure 3: Photos of the SAPP test in the TVAC Chamber with and without Closeout Blanketing

C. Warm Zone Configuration

The warm zone (Figure 4 left) was designed to simulate the internal conductive and radiative environment of the LEMS bus assembly during lunar night. The radiative and conductive sinks have independent control so that their individual contributions to the total heat loss could be characterized. It consisted of a bus plate, a chiller plate, and a surrounding warm box.

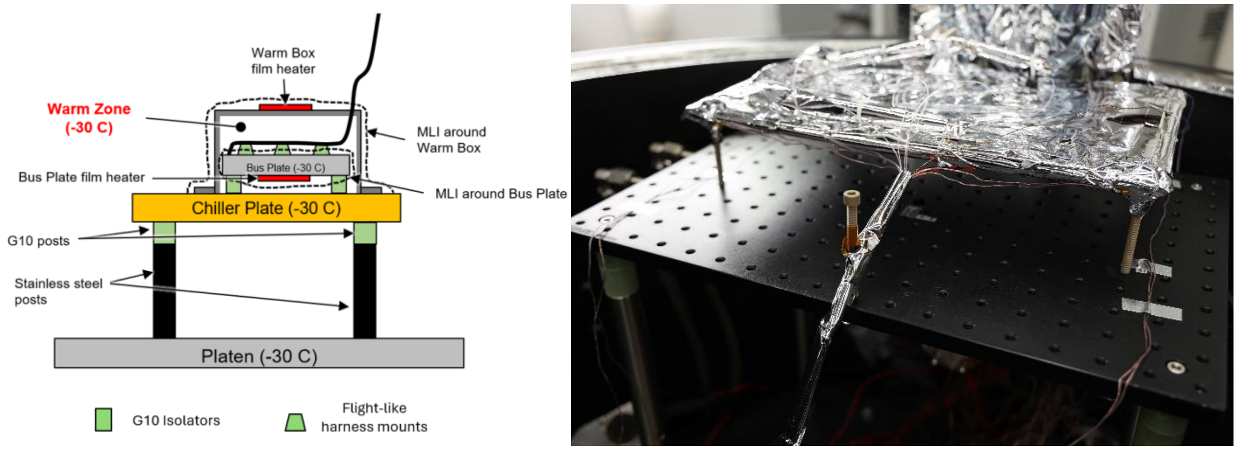

Figure 4: (left) Warm zone configuration. (right) As-built bus plate mounting showing Polyether Ether Ketone (PEEK) bolts.

The Bus Plate was an aluminum mounting plate that created the interface temperature sink for the internal SAPP harness segments. Burnished aluminum tape was used to attach the SAPP harness to the bus plate. The plate temperature was actively controlled via a 43-Ω film heater and monitored using a calibrated silicon diode (SD) and thermocouples distributed across the surface to capture potential temperature gradients.

As the SAPP conductive sink, the Bus Plate was mounted to a plumbed chiller Plate using 3 inch long ¼”-20 machine screws with support nuts to isolate from the chiller plate. Figure 4 shows the as-built bus plate mounting. The chiller Plate was driven by a circulating fluid line, providing temperature control of the warm zone structure. The PEEK bolts increased the thermal resistance between the bus plate and chiller plate, thereby minimizing heat flow error. SDs on the chiller plate and bus plate provide temperature input to the relevant heater controllers that can zero-out heat flow between the chiller plate and bus plate. These features ensure that the SAPP harness is the dominant heat transfer path from the Bus Plate to the cryopanel.

A five-sided, black-anodized aluminum warm box was mounted around the bus plate to the chiller plate to simulate the internal radiative sink of the flight configuration. The interior surface was black anodized so that any radiation heat transfer was greater than what is expected in flight. The warm box temperature was independently controlled using an additional 43-Ω film heater. Exterior warm box surfaces were blanketed with MLI to reduce temperature gradients induced by the cold chamber shroud.

D. Cold Zone Configuration

The primary cold boundary was an aluminum Cryopanel driven by the first stage of a two-stage cryocooler. Five independently controlled bar heaters (219 Ω-227 Ω) were distributed across the Cryopanel surface to enable precise temperature control and uniformity. The SAPP wire ends are stripped of their insulation and taped to the Cryopanel with burnished aluminum tape to sink them down to the boundary temperature. A calibrated SD and thermocouples were distributed across the Cryopanel surface to verify temperature uniformity and quantify gradients.

The Cryopanel was blanketed with MLI to reduce radiation exchange with the chamber shroud and reduce temperature gradients along the Cryopanel. Independent shroud temperature control allowed radiative boundary conditions to be adjusted in selected balance cases to evaluate the contribution of external radiation heat transfer to total SAPP heat leak.

E. Instrumentation and Boundary Control

The test setup was instrumented with calibrated SDs and Type T thermocouples distributed across the Bus Plate, SAPP harness, Cryopanel, warm box, and supporting hardware (Figure 5). Sensors were positioned at harness tie-down points, along representative harness segments, at thermal sink interfaces, and beneath MLI layers. This distribution enabled characterization of axial temperature gradients along the harness and verification of boundary condition uniformity. Table 2 captures the manufacturer-reported errors from the power supplies, power monitors, and temperature monitors used for monitoring the test sensors and controlling test sensors.

Table 2: Ground support equipment description and systematic error

No.	Supplier	Model	Description	Component	Error [V]	Error [A]	Sensor & Monitor Error [°C
1	Nat. Inst.	PXIe-4353	Temperature Monitor	Payload TCs	0.0025	-	1.005
2	Nat. Inst.	PXIe-4353	Temperature Monitor	Payload TCs	0.0025	-	1.005
3	Nat. Inst.	PXIe-4353	Temperature Monitor	Facility TCs	0.0025	-	1.005
4	Nat. Inst.	PXIe-4353	Temperature Monitor	Facility TCs	0.0025	-	1.005
5	Lakeshore	336	SD & Heater Controller	Payload SDs	-	-	0.098
6	Lakeshore	336	SD & Heater Controller	Payload SDs	-	-	0.098
7	Keithley	2460	Source measure unit	Bus plate Htr	0.015% + 5 mV	0.020% + 10 µA	-
8	Keithley	2460	Source measure unit	Warm box Htr	0.015% + 5 mV	0.020% + 10 µA	-
9	Keithley	2280S-60-3	Precision measurement DC supply	Cryopanel Htrs	0.02% + 4 mV	0.05% + 250 µA	-
10	Keithley	2280S-60-3	Precision measurement DC supply	Cryopanel Htrs	0.02% + 4 mV	0.05% + 250 µA	-
11	Keithley	2280S-60-3	Precision measurement DC supply	Cryopanel Htrs	0.02% + 4 mV	0.05% + 250 µA	-
12	Keithley	2280S-60-3	Precision measurement DC supply	Cryopanel Htrs	0.02% + 4 mV	0.05% + 250 µA	-
13	Keithley	2280S-60-3	Precision measurement DC supply	Cryopanel Htrs	0.02% + 4 mV	0.05% + 250 µA	-

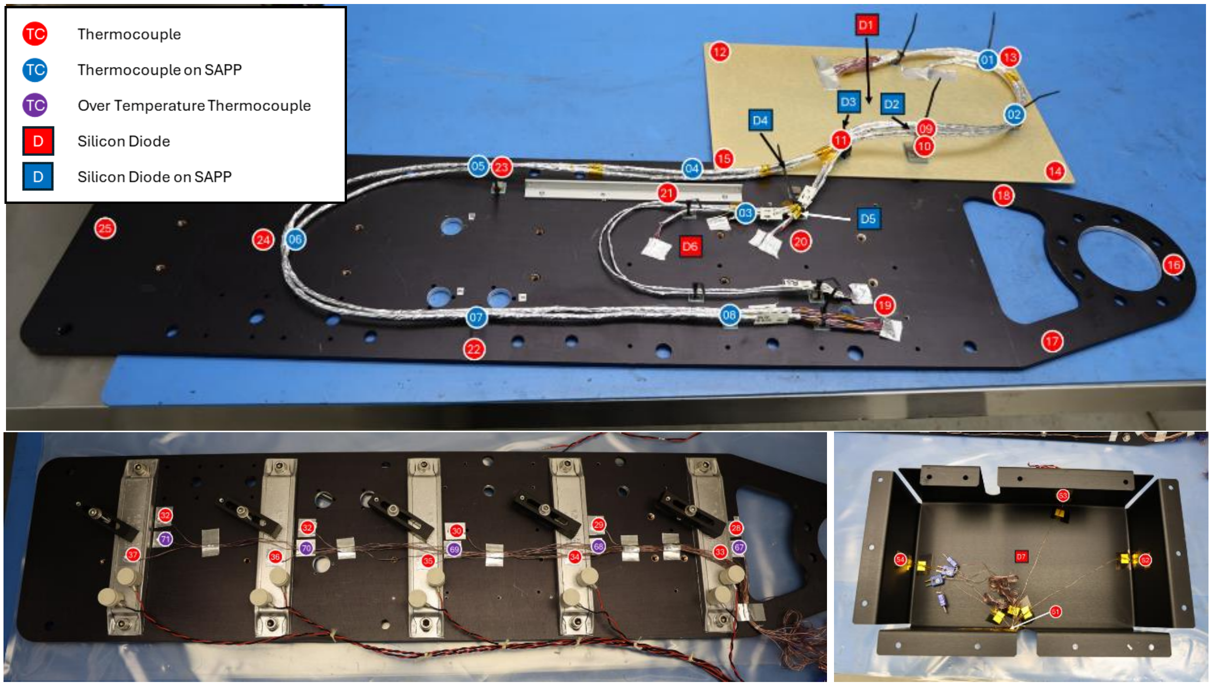

Figure 5: (upper) Test sensors on Cryopanel front, Bus Plate, and SAPP RRU. (bottom left) Test sensors on Cryopanel rear. (bottom right) Test sensors on warm box.

All heaters (Figure 5 and Figure 6) were independently controlled in proportional temperature control mode. Heater voltages and currents were continuously recorded for evaluating balance stability and correlating the thermal model. During balances where the temperature of the bus plate equals the temperature of the chiller plate and warm box, the heat loss through the SAPP is the power of heater #7.

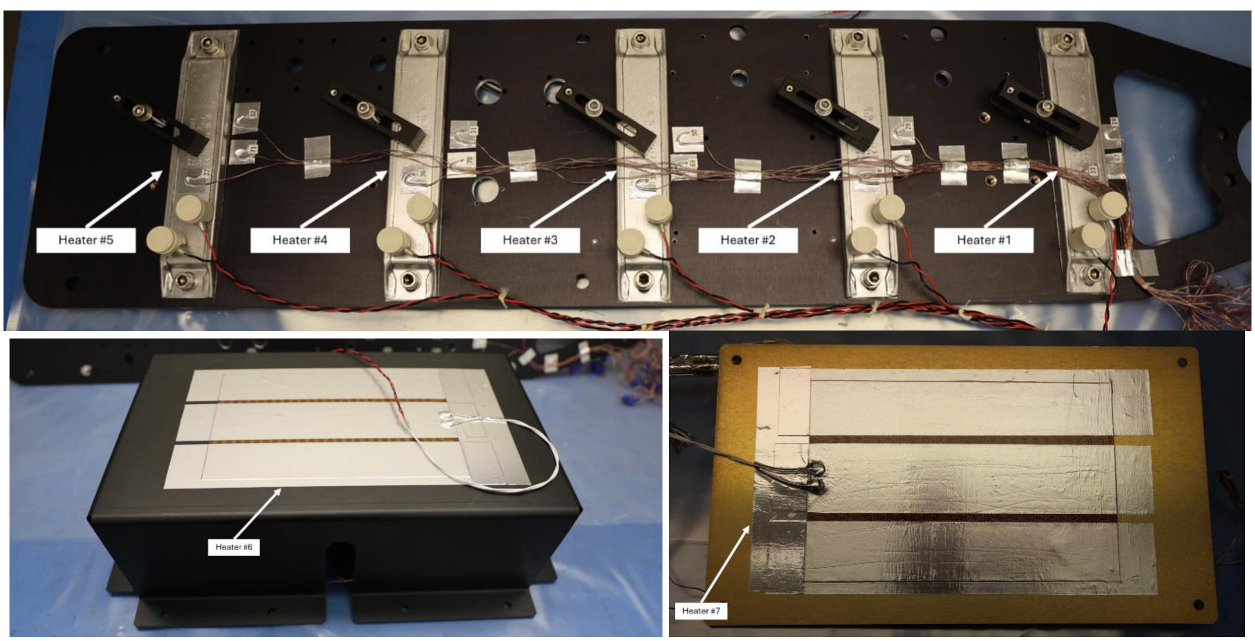

Figure 6: (upper) Cryopanel bar heaters. (bottom left) warm box heater. (bottom right) Bus Plate heater.

F. Flight-Like SAPP Harness Materials and Standoffs

The SAPP harness is a mix of gauges and materials designed to minimize the thermal conductance while meeting electrical requirements like power, signal quality, and grounding. For high-current wires, like the solar array power lines, copper was selected. All other wires which carry low-current signals are made from manganin. Both conductors are insulated with Teflon and supported on insulating standoffs between the wire terminations. Table 3 summarizes wire material, gauge, and number of units used in the SAPP harness.

Table 3: SAPP harness wire list

Gauge (AWG)	Termination	Material	No.
30	Temperature Sensors, Activation Switches, Seismometer Signals	Manganin	50
28	Solar Array Power	Copper	8
30	Seismometer Power	Copper	12
30	Ground	Copper	2

In addition to low thermal conductivity wires, the SAPP heat loss was further minimized by maximizing the conductor length. The harness was secured to the structure with Ultem 1000 thermally insulating standoffs like the ClickBond CB9302, ClickBond CB9257 (a.k.a ClickBond tree), and two types of custom mounts (Figure 7). After it was wrapped with MLI, the SAPP was tied to the relevant mount with lacing chord. The standoffs were placed so that the distances between standoffs was the same as in-flight.

Figure 7: SAPP standoffs for tiedowns. (left to right) ClickBond CB9302, ClickBond CB9257, custom external, custom internal

The MLI insulating the SAPP was constructed from two layups. The SAPP attached to the bus plate standoffs is wrapped with a 6 layers of double-sided aluminized interspersed with Dacron mesh. The inner and outer surfaces are vapor deposited aluminum. The SAPP MLI attached to the cryocooler is a similar layup except the outer layer is a laminate of Stamet and NEXTEL ballistic fabric with the Stamet facing out.

G. Test Profile

The thermal vacuum test profile was structured to obtain mission-representative heat leak data while systematically varying boundary conditions to support model correlation. The test consisted of a bakeout followed by four thermal balance points. Each balance case varied a single boundary condition relative to the baseline configuration in order to isolate conductive and radiative sensitivities. The overall profile is shown below in Figure 8.

The first balance captured the measurement of the SAPP harness heat loss while the subsequent balances varied the external environment boundary conditions to determine their relative contributions to the heat loss. Following a bakeout, balance #1 established the nominal lunar night configuration. The Cryopanel was controlled to the cold external sink temperature, while the bus plate, warm box, chiller plate, and chamber platen were maintained at the flight internal bus temperature (-30 °C). The chamber shroud was held at the coldest background temperature possible, approximately -180 °C. TB 1 provided the primary data set for total SAPP cold operational heat leak.

Balance #2 increased the warm zone boundary temperature by 10 °C relative to Balance #1 while maintaining the same cold external sink. This increased the temperature gradient across the harness and provided conductance sensitivity data. TB 2 supported evaluation of how internal heater setpoint adjustments would affect heat leak and battery demand and provided an additional condition for model correlation.

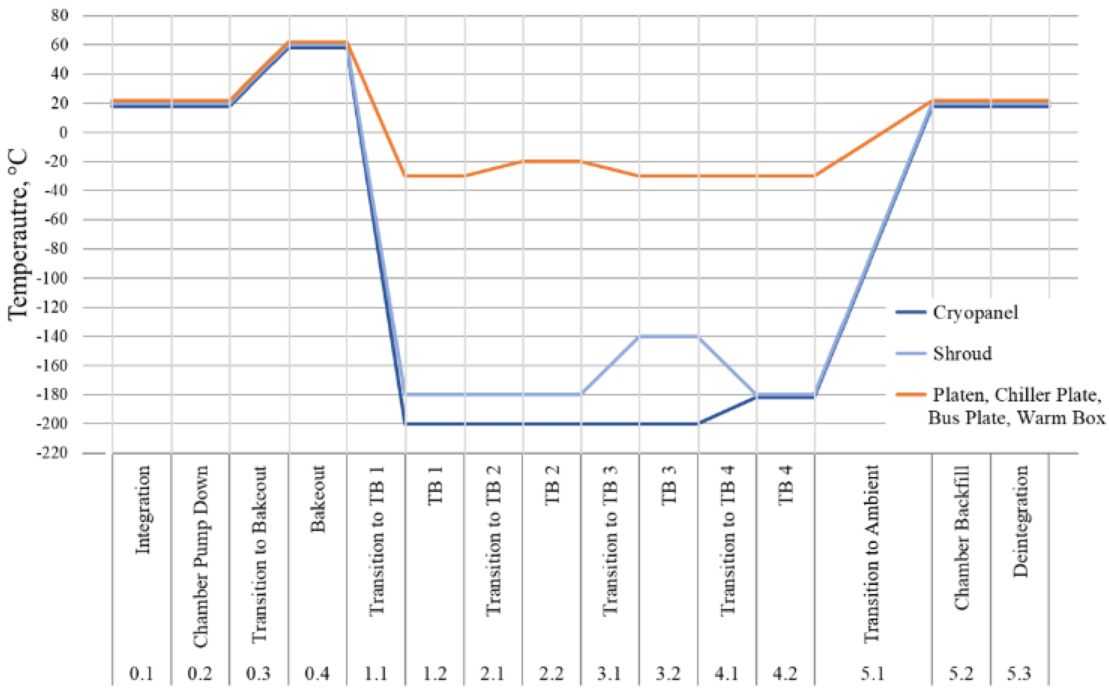

Figure 8: Test Profile

Balance #3 maintained the conductive boundary temperatures of Balance #1 but increased the chamber shroud temperature. This modified the effective radiative environment without changing the Cryopanel conductive sink. Balance # 3 therefore enabled separation of conductive and radiative contributions and informed tuning of radiative parameters in the thermal model.

Finally, balance #4 adjusted the Cryopanel temperature while maintaining nominal internal boundary temperatures. This reduced the overall temperature gradient across the harness and provided heat leak data at a different mean temperature.

III. Test Results

Figure 9 shows the as-run test profile temperatures and Table 4 lists the sample periods for each of the balances. Balance periods were chosen from the test data such that the temperature and heater power data showed rates of change less than 0.1°C/h and 0.01 W/h, respectively. The length of the sample period had to be at least four hours to ensure adequate data gathering. Most of the cycles fell on one or two day periods such that the test could be left overnight for long periods of balance stability.

Table 4: Balance Measurement Sample Start, End, and Duration

Test Phase	Start	End	Duration [h]	No. Samples (N)
Balance #1	09/16/2025 05:00	09/16/2025 11:00	6	720
Balance #2	09/16/2025 18:00	09/17/2025 06:00	10	1200
Balance #3	09/17/2025 18:00	09/18/2025 08:00	12	1440
Balance #4	09/18/2025 14:00	09/18/2025 18:00	4	480

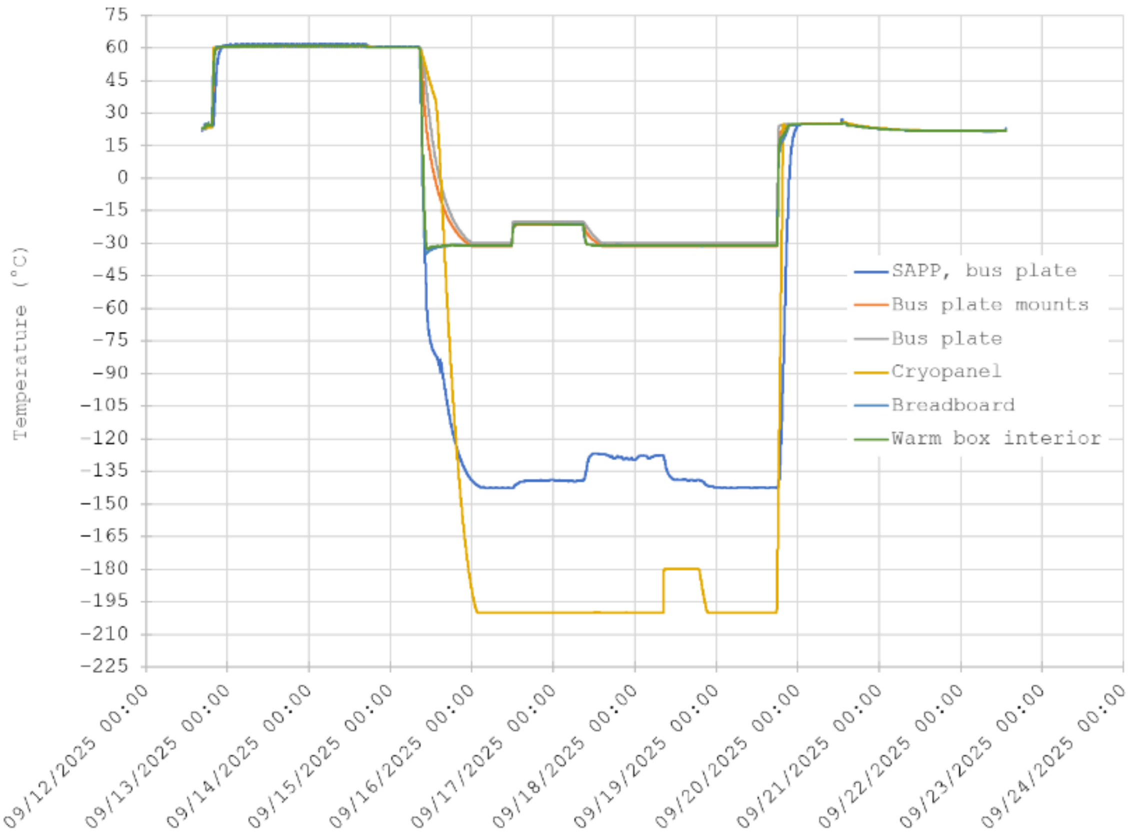

Figure 9: As-Run Test Profile

Table 5 lists the temperature results for selected sensors relevant to the SAPP heat loss measurement and to model correlation. The error calculation is the manufacturer-reported systematic error assumed to be three standard deviations combined via quadrature with the random noise error from the measurements at three standard deviations. The equations for error propagation are included in the Appendix. The sensors and power monitors have a minimum value which is the systematic error because many sensors had little contribution from random noise. The SDs have an error an order of magnitude less than the thermocouples which lends high confidence to determining errant heat flows in the GSE.

In Balance #1 and Balance #2 SD-01, SD-07, and SD-08 show that the warm zone GSE is nearly equal in temperature and should have little to no heat loss from the bus plate except along the SAPP harness. However, the thermocouples show a small gradient so a simple conduction and radiation model was developed to determine the error resulting from heat flows to the warm box and chiller plate from the bus plate. This is presented in the next section.

Table 5: Balance Average Temperature Measurements

Temperature Sensor		Temperature Measurement ± 3σ Error [°C]			
Label	**Description**	**Balance #1**	**Balance #2**	**Balance #3**	**Balance #4**
SD-01	Bus plate, center	-30.0 ± 0.089	-20.0 ± 0.089	-30.0 ± 0.089	-30.0 ± 0.089
SD-02	SAPP at tie down #4	-73.3 ± 0.089	-64.6 ± 0.089	-69.2 ± 0.090	-71.9 ± 0.089
SD-03	SAPP at tie down #5	-88.8 ± 0.089	-81.4 ± 0.089	-83.4 ± 0.091	-86.7 ± 0.089
SD-04	SAPP at tie down #11	-104.0 ± 0.089	-97.9 ± 0.089	-96.1 ± 0.093	-102.1 ± 0.090
SD-05	SAPP at tie down #6	-107.7 ± 0.089	-101.7 ± 0.089	-101.0 ± 0.092	-104.5 ± 0.089
SD-06	Cryopanel	-203.1 ± 0.089	-203.0 ± 0.089	-203.0 ± 0.089	-182.3 ± 0.089
SD-07	Warm box	-30.0 ± 0.089	-20.0 ± 0.089	-30.0 ± 0.089	-30.0 ± 0.089
SD-08	Chiller plate, top center	-30.1 ± 0.089	-20.0 ± 0.089	-30.0 ± 0.089	-30.0 ± 0.089
SD-09	Cryocooler, second stage	-254.8 ± 0.089	-253.1 ± 0.089	-253.1 ± 0.089	-253.1 ± 0.089

Temperature Sensor		Temperature Measurement ± 3σ Error [°C]			
Label	**Description**	**Balance #1**	**Balance #2**	**Balance #3**	**Balance #4**
TC-01	SAPP at tie down #2	-47.3 ± 1.005	-37.8 ± 1.005	-45.6 ± 1.005	-46.5 ± 1.005
TC-02	SAPP at tie down #3	-58.4 ± 1.005	-49.3 ± 1.005	-55.6 ± 1.005	-57.3 ± 1.005
TC-03	SAPP at tie down #7	-122.7 ± 1.005	-118.1 ± 1.005	-114.6 ± 1.005	-118.9 ± 1.005
TC-04	SAPP at tie down #12	-131.3 ± 1.005	-127.5 ± 1.005	-118.5 ± 1.006	-129.0 ± 1.005
TC-05	SAPP at tie down #15	-144.3 ± 1.005	-141.4 ± 1.005	-128.9 ± 1.007	-141.7 ± 1.005
TC-06	SAPP between tie down #15/16	-150.1 ± 1.005	-147.5 ± 1.005	-133.2 ± 1.007	-147.0 ± 1.005
TC-07	SAPP at tie down #16	-153.0 ± 1.005	-150.4 ± 1.005	-136.1 ± 1.007	-149.3 ± 1.005
TC-08	SAPP at tie down #17	-153.7 ± 1.005	-150.6 ± 1.005	-139.5 ± 1.006	-147.8 ± 1.005
TC-09	Tree (tie down #4) top	-33.2 ± 1.005	-23.3 ± 1.005	-32.8 ± 1.005	-33.0 ± 1.005
TC-10	Tree (tie down #4) bottom	-29.9 ± 1.005	-20.0 ± 1.005	-29.9 ± 1.005	-29.9 ± 1.005
TC-11	Finale (tie down #5) bottom	-31.1 ± 1.005	-21.3 ± 1.005	-31.0 ± 1.005	-31.0 ± 1.005
TC-47	Chiller, top, right corner	-31.8 ± 1.005	-22.2 ± 1.005	-31.7 ± 1.005	-31.7 ± 1.005
TC-48	Chiller, top, left corner	-30.2 ± 1.005	-20.3 ± 1.005	-30.1 ± 1.005	-30.1 ± 1.005
TC-49	Chiller, rear, left corner	-30.2 ± 1.005	-20.3 ± 1.005	-30.1 ± 1.005	-30.0 ± 1.005
TC-50	Chiller, rear, right corner	-31.6 ± 1.005	-21.9 ± 1.005	-31.5 ± 1.005	-31.5 ± 1.005
TC-51	Warm box interior, front face	-30.7 ± 1.005	-21.0 ± 1.005	-30.6 ± 1.005	-30.6 ± 1.005
TC-52	Warm box interior, left face	-30.6 ± 1.005	-20.9 ± 1.005	-30.5 ± 1.005	-30.5 ± 1.005
TC-53	Warm box interior, rear face	-31.0 ± 1.005	-21.3 ± 1.005	-30.9 ± 1.005	-30.9 ± 1.005
TC-54	Warm box interior, right face	-31.7 ± 1.005	-22.0 ± 1.005	-31.5 ± 1.005	-31.6 ± 1.005
AVG1	Bus Plate TC Avg	-29.9 ± 1.005	-19.9 ± 1.005	-29.8 ± 1.005	-29.8 ± 1.005
AVG2	Cryopanel TC Avg	-200.1 ± 1.005	-200.1 ± 1.005	-199.9 ± 1.005	-180.0 ± 1.005
AVG3	Breadboard / Chiller Plate TC Avg	-30.9 ± 1.005	-21.1 ± 1.005	-30.8 ± 1.005	-30.8 ± 1.005
AVG4	warm box TC Avg	-31.0 ± 1.005	-21.3 ± 1.005	-30.9 ± 1.005	-30.9 ± 1.005
AVG5	Platen TC Avg	-29.7 ± 1.005	-19.8 ± 1.005	-29.7 ± 1.005	-29.7 ± 1.005
AVG6	Chamber Shroud TC Avg	-181.1 ± 1.028	-180.9 ± 1.016	-141.2 ± 1.022	-181.4 ± 1.043

Table 6: Balance Average Heater Power Measurements

Unit No.	Description	Heater Power ± 3σ Error [W]			
		Balance #1	**Balance #2**	**Balance #3**	**Balance #4**
7	Bus plate heater	0.117 ± 3.0E-04	0.124 ± 2.9E-04	0.107 ± 2.7E-04	0.113 ± 2.8E-04
8	Warm box heater	1.685 ± 1.5E-03	1.929 ± 1.6E-03	1.545 ± 1.3E-03	1.611 ± 1.4E-03
9	Cryopanel heaters	OFF	OFF	OFF	11.386 ± 1.9E-02
10	Cryopanel heaters	6.000 ± 1.2E-02	6.714 ± 1.3E-02	6.837 ± 1.3E-02	5.834 ± 1.2E-02
11	Cryopanel heaters	1.274 ± 1.6E-02	1.359 ± 1.2E-02	1.395 ± 1.1E-02	2.296 ± 4.3E-02

The measurement uncertainty of the SDs and power supplies gives confidence that the power measurement of the bus plate heater during Balance #1 at 0.117 W (Table 6) flows mostly out of the SAPP harness. Assuming a simple linear conductance model, the power measurement indicates the harness has a thermal conductance of 6.9E-04 W/°C when the bus plate is at -30.0°C (SD-01) and the cryopanel (AVG1) is at -200.1°C. This is a 48% reduction in the flight predicts of the SAPP harness heat loss and thermal conductance. However, uncertainty in the temperature measurements can hide heat flows that increase the thermal conductance measurement.

IV. Thermal Model Correlation

A. Thermal Model

A simple resistor-network thermal model was developed to determine the SAPP heat flow error bounds that can result from uncertainty in the temperature measurements. The major contributor to the uncertainty is heat flows from the bus plate to the chiller plate. There is additional uncertainty for potential infrared radiation heat flows from the bus plate to the chiller plate and warm box but these are negligible given the measured temperature gradients. The resistor network model is shown in Figure 10.

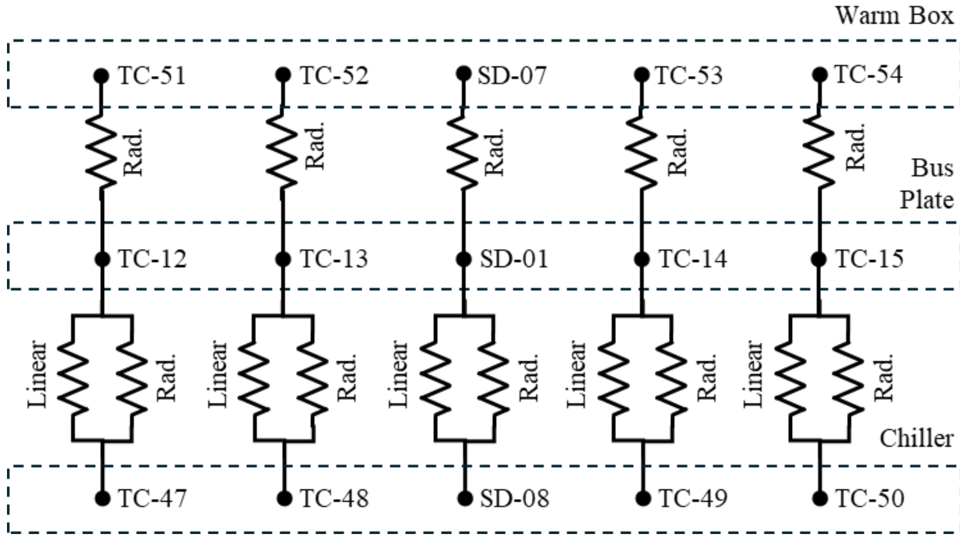

Figure 10: Simple resistor network to evaluate the heat flow error due to temperature uncertainty

The bus plate is supported above the chiller plate by four 0.076 m (3 in) ¼"-20 PEEK bolts as seen in Figure 4 (right). For a conservative estimate of the potential heat flow along these bolts, the length of the conduction is reduced from 0.076 m (3 in) to 0.0508 m (2 in). The conductivity for PEEK is assumed to be 0.26 W/m/K. From these values, the conductance for each PEEK bolt is estimated to be 3.6E-04 W/°C.

An example of the error for PEEK bolt heat flow between TC 12 and TC 47 is shown using Eq. (1). It is the sum of the error associated with the measured temperature gradient and the measurement uncertainty of the thermocouples. Table 7 shows the relevant sensor measurements for Balance #1 and calculates the error for each of the PEEK bolts.

$$conduction\ error = 0.00036 * (TC_{12} - TC_{47} + \sqrt{\sigma_{TC12}^2 + \sigma_{TC47}^2}) \tag{1}$$

The radiative contribution to the heat flow error is calculated as the maximum difference in temperature between the bus plate and the warm box or the chiller plate. There are five sensors on the bus plate, four thermocouples and one silicon diode, so the area of the bus plate is divided equally into five parts. This is a total plate area of 0.072 m^2 (112 in^2) which gives each sensor an area of 0.014 m^2 (22.4 in^2). The bus plate is blanketed with 6-layer MLI with aluminized outer surface which is assumed to have a maximum infrared emissivity of 0.05. For conservatism, the warm box and chiller are assumed to be black bodies. For the sample calculation of the heat error given by Eq. (2), the temperatures are biased plus or minus the sensor error so that the gradient is maximized. The radiation error is calculated for each sensor individually and is presented in Table 7 for Balance #1.

$$radiation\ error = (0.014)(0.05)(5.67 * 10^{-8})(TC_{12}^4 - TC_{47}^4) \tag{2}$$

Table 7: Bus plate conductive and radiative heat flow uncertainty from TC measurements

Label	Sensors for Delta	Temperature Delta (Bus Plate - Boundary) [°C]	Heat Flow Error [W]	
			Linear	Radiative
Bus plate to chiller	SD-01 - SD-08	0.1 ± 0.126	0.000	0.001
	TC-12 - TC-47	1.7 ± 1.421	0.001	0.009
	TC-13 - TC-48	0.4 ± 1.421	0.001	0.006
	TC-14 - TC-49	0.1 ± 1.421	0.001	0.005
	TC-15 - TC-50	1.7 ± 1.421	0.001	0.009
Bus plate to warm box	SD-01 - SD-07	0.0 ± 0.126	-	0.000
	TC-12 - TC-51	0.6 ± 1.421		0.006
	TC-13 - TC-52	0.8 ± 1.421		0.007
	TC-14 - TC-53	0.9 ± 1.421		0.007
	TC-15 - TC-54	1.8 ± 1.421		0.009
Heat Flow Error Subtotal			0.004	0.057
Total Heat Flow Error			0.061	

The total heat flow error has been determined to be 0.061 W. From the test data presented in Section III the measured heat flow and uncertainty for Balance #1 is 0.117 ± 0.061 W. Because the errors propagated have been at least three standard deviations, the test results and analysis show that the SAPP heat loss is less than 0.178 W with 99.8% confidence. Given the test goal was to measure the heat flow to less than 0.223 W, the SAPP harness and conductance test meet requirements with 0.045 W or 21% of margin.

Similarly, the conductance error has been determined to be 3.6E-04 W/°C. From the test data presented in Section III the measured SAPP thermal conductance and uncertainty for Balance #1 is 6.9E-04 ± 3.6E-04 W/°C. Therefore, the SAPP conductance is less than 1.05E-03 W/°C. with 99.8% confidence.

V. Conclusion

The thermal conductance test of the SAPP harnessing was able to measure the heat loss and conductance to within test objectives in a flight-like configuration and environment. Systematic and random errors were propagated to build a confidence interval of at least three standard deviations. The heat leak was determined to be 0.117 ± 0.061 W and the thermal conductance was determined to be 6.9E-04 ± 3.6E-04 W/°C. These measurements give the LEMS project high confidence that the SAPP harness design will meet its design performance.

Further work is needed to finalize the second and third objectives of the test. A detailed thermal model has yet to be correlated due to project schedule constraints. The work is planned for the future. This more detailed model being developed in Thermal Desktop should reduce the uncertainty in the radiative heat flow error between the bus plate and other test GSE. Knowledge of the conductive properties of the aluminum bus plate, warm box, and chiller plate; and applied heater power should allow the silicon diode to inform on the accuracy of the thermocouple measurements.

The detailed model should also be able to estimate the conductance of the various standoffs used to support the SAPP on the bus plate and the chiller plate. Pre-test modeling assumed that the harness had perfect contact to the top of the standoff and that all thermal resistance is in the standoff. Since the heat flow measurement was lower than expected, the imperfect contact of the lacing chord over MLI that secures the SAPP harness to the standoff could be increasing the thermal resistance significantly. Another potential cause of the lower heat loss can be the effective emissivity, or estar, of the SAPP MLI blanketing.

VI. Appendix – Error Propagation

To ensure accurate measurement of boundary temperatures, harness temperatures, and heater power, sensor and monitor errors were tabulated and propagated. The presented errors are the quadrature of the systematic and random errors from the hardware and data, respectively.

1. *Silicon Diode*

$$SD\ Error = 0.089^2 + 3\sqrt{\frac{\sum(x_i - \bar{x})^2}{N}} \tag{3}$$

2. *Thermocouple*

$$TC\ Error = 1.005^2 + 3\sqrt{\frac{\sum(x_i - \bar{x})^2}{N}} \tag{4}$$

3. *Thermocouple Average*

Because much of the error present in the thermocouple reading is systematic, averaging does not significantly reduce the error of a single sensor.

$$Average\ TC\ Error = \sqrt{\frac{\sum(TC\ Error_i)^2}{No.\ Sensors}} \tag{5}$$

4. *Bus Plate and warm box Heater Power*

$$Voltage\ Error = \sqrt{(0.00015\bar{V} + 0.005)^2 + 3\sqrt{\frac{\sum(V_i - \bar{V})^2}{N}}} \tag{6}$$

$$Current\ Error = \sqrt{(0.0002\bar{I} + 0.00001)^2 + 3\sqrt{\frac{\sum(I_i - \bar{I})^2}{N}}} \tag{7}$$

$$Power\ Error = \sqrt{(Voltage\ Error)^2 + (Current\ Error)^2} \tag{8}$$

5. *Cryopanel Heater Power*

$$Voltage\ Error = \sqrt{(0.0002\bar{V} + 0.004)^2 + 3\sqrt{\frac{\sum(V_i - \bar{V})^2}{N}}} \tag{9}$$

$$Current\ Error = \sqrt{(0.0005\bar{I} + 0.00025)^2 + 3\sqrt{\frac{\sum(I_i - \bar{I})^2}{N}}} \tag{10}$$

$$Power\ Error = \sqrt{(Voltage\ Error)^2 + (Current\ Error)^2} \tag{11}$$

6. *Bus Plate to Chiller Plate Heat Flow*

The radiation error is derived from the general error propagation equation using partial derivatives

$$Current\ Error = \sqrt{(0.0005\bar{I} + 0.00025)^2 + 3\sqrt{\frac{\sum(I_i - \bar{I})^2}{N}}} \tag{12}$$

$$Power\ Error = \sqrt{(Voltage\ Error)^2 + (Current\ Error)^2} \tag{13}$$

VII. Acknowledgments

The authors of this paper would like to acknowledge the LEMS-A3 project for financial support. Special thanks to the engineers and technicians of the NASA GSFC Thermal Technology Development and Demonstration Facility for their support in designing, preparing, and conducting this test.

VIII. References

[1] E. Burbridge and J. Rodriguez-Ruiz, "Artemis 3 Lunar Environment Monitoring Station (LEMS-A3) Thermal Control Subsystem Architecture," in *International Conference on Environmental Systems*, Prague, Czechia, 2025.

IX. Manuscript Submission Checklists

[Note: this page should be deleted before final manuscript submission]

1. First Draft Manuscript checklist
    - □ File is .docx format
    - □ Line numbers are visible along the left hand margin
    - □ Paper number is located in the upper right corner of the headers
    - □ Conference details are located in the upper left corner of the headers
    - □ Abstract matches easychair content (note that Easychair can be updated if needed)
    - □ Authors and affiliations match easychair authors (note that Easychair can be updated if needed)
    - □ Title matches easychair title (note that Easychair can be updated if needed)
    - □ Paper length (including references and appendices, but excluding this page) is 15 pages or fewer.
    - □ All content is included (paper will be rejected if only partially complete)

2. Second Draft Manuscript

    Note that Second drafts are only required if your first draft manuscript received one or more scores of 0 or lower. If all scores from reviewers were 1, 2, or 3, please proceed to the final manuscript
    - □ File is .docx format
    - □ Line numbers are visible along the left hand margin
    - □ Paper number is located in the upper right corner of the headers
    - □ Conference details are located in the upper left corner of the headers
    - □ Abstract matches easychair content (note that Easychair can be updated if needed)
    - □ Authors and affiliations match easychair authors (note that Easychair can be updated if needed)
    - □ Title matches easychair title (note that Easychair can be updated if needed)
    - □ Paper length (including references and appendices, but excluding this page) is 15 pages or fewer.
    - □ Changes from the first draft are tracked so reviewers can see where their comments have been addressed.

3. Final Manuscript
    - □ File is .pdf format
    - □ Line numbers are removed
    - □ Paper number is located in the upper right corner of the headers
    - □ Conference details are located in the upper left corner of the headers
    - □ Abstract matches easychair content (note that Easychair can be updated if needed)
    - □ Authors and affiliations match easychair authors (note that Easychair can be updated if needed)
    - □ Title matches easychair title (note that Easychair can be updated if needed)
    - □ Paper length (including references and appendices, but excluding this page) is 15 pages or fewer.
    - □ This page is removed after confirming all content above is included and accurate.